January 2009

Normal stiffness calibration of microfabricated tri-layer conducting polymer actuators

Michael J. Higgins
University of Wollongong, mhiggins@uow.edu.au

Gursel Alici
University of Wollongong, gursel@uow.edu.au

Normal stiffness calibration of microfabricated tri-layer conducting polymer actuators

Abstract

This paper reports on the stiffness characterization of microfabricated tri-layer conducting polymer (PPy) actuators. The rectangular, polypyrrole microactuators, which could operate both in aqueous and non-aqueous media, were fabricated using an excimer laser ablation technique that provided high throughput production and did not require cleanroom facilities. The microactuators were fixed at one end with electrical contacts and the other was end free to act as an electroactive microcantilever beam. An atomic force microscope (AFM) was used to measure the microactuator deflection under a range of normal forces applied by the AFM cantilever. A modified reference spring constant calibration method was employed to determine the stiffness constants of the microactuators. The stiffness of the microactuators in the electroactive (electrically stimulated) and passive state (no stimulation) were evaluated separately and compared. In doing so, the study presents results leading to the stiffness characterization of the first air-operated polymer microactuators and implementation of a simple, reliable and effective method for directly measuring the spring constant of polymer microactuators. This method is an alternative to the use of mechanical modeling methods, which can be difficult to implement for multi-layer (composite) polymer actuators. Importantly, our results highlight several requirements for using the reference spring method to accurately determine stiffness values of any microcantilever generally fabricated from soft, deformable materials.

Keywords

stiffness, calibration, microfabricated, normal, tri, actuators, layer, conducting, polymer

Disciplines

Life Sciences | Physical Sciences and Mathematics | Social and Behavioral Sciences

Normal stiffness calibration of microfabricated tri-layer conducting polymer actuators

2009 Smart Mater. Struct. 18 065013

(http://iopscience.iop.org/0964-1726/18/6/065013)

Smart Mater. Struct. **18** (2009) 065013 (9pp) doi:10.1088/0964-1726/18/6/065013

Normal stiffness calibration of microfabricated tri-layer conducting polymer actuators

Gursel Alici[1] **and Michael J Higgins**[2]

[1] School of Mechanical, Materials and Mechatronic Engineering, University of Wollongong, Australia
[2] Intelligent Polymer Research Institute, University of Wollongong, Australia

Received 22 January 2009, in final form 26 March 2009
Published 6 May 2009
Online at stacks.iop.org/SMS/18/065013

Abstract
This paper reports on the stiffness characterization of microfabricated tri-layer conducting polymer (PPy) actuators. The rectangular, polypyrrole microactuators, which could operate both in aqueous and non-aqueous media, were fabricated using an excimer laser ablation technique that provided high throughput production and did not require cleanroom facilities. The microactuators were fixed at one end with electrical contacts and the other was end free to act as an electroactive microcantilever beam. An atomic force microscope (AFM) was used to measure the microactuator deflection under a range of normal forces applied by the AFM cantilever. A modified reference spring constant calibration method was employed to determine the stiffness constants of the microactuators. The stiffness of the microactuators in the electroactive (electrically stimulated) and passive state (no stimulation) were evaluated separately and compared. In doing so, the study presents results leading to the stiffness characterization of the first air-operated polymer microactuators and implementation of a simple, reliable and effective method for directly measuring the spring constant of polymer microactuators. This method is an alternative to the use of mechanical modeling methods, which can be difficult to implement for multi-layer (composite) polymer actuators. Importantly, our results highlight several requirements for using the reference spring method to accurately determine stiffness values of any microcantilever generally fabricated from soft, deformable materials.

(Some figures in this article are in colour only in the electronic version)

1. Introduction

Electroactive polymers (EAP) are considered to be a potential alternative to conventional actuators due to their attractive properties, including minimal electric power consumption, light weight and compliant properties, biocompatibility, ability to operate in air and fluid, insensitivity to magnetic fields and simple fabrication. Furthermore, the scaling down of these EAP to the micron level greatly improves their actuation properties such as the blocking or peak force. In recognition of the potential applications of EAP, a wealth of studies have been conducted on organic conducting polymer (OCP) actuators, including ionic and non-ionic systems, to assess their suitability for use at the macro-down to the nanometer level. The use of OCP across these dimensions amounts to numerous applications, including the micromanipulation of living cells, bio-analytical nanosystems, data storage, lab-on-chip, microvalve, microswitch, micropump, microshutter, cantilever light modulators, micro-optical instrumentation, artificial muscles for macro-robotics and so on.

The actuator materials currently used for micro-electro-mechanical systems (MEMS) have been found to be suitable in most cases except those involving interactions with the environment, such as the ability to mechanically grasp and hold an object (e.g. gripping). In terms of the latter, actuators made from inorganic materials face two key problems: (1) the implementation of large design footprints or areas and (2) the brittleness of the material. Conventional actuators suffer from relatively large footprints that limit the degree of miniaturization and actuator density. In contrast, polymer

thermal actuators have been fabricated into arrays to achieve high actuator densities [1], and as such their parallel arrangements can be exploited for high power applications like the handling of large objects. The brittleness of inorganic materials means that they readily break upon contact with macroscale objects. Polysilicon micro-grippers have been known to break if touched by a macro-object or if exposed to air velocities higher than 1 $\mathrm{m\,s^{-1}}$ [2]. In contrast, the compliant properties of the polymer actuators allow the resumption of normal operation after the actuator has been subject to significant mechanical forces or disturbance [3]. By incorporating electroactive polymers in MEMS, the fabrication of the actuator elements is simplified, for example, simple EAP coatings can replace complex interdigitated comb drives and multi-layer piezo systems. Furthermore, their use in MEMS brings new functionality not available in silicon-based systems, including their larger actuation at lower voltages, operation in air and wet media, biocompatibility, and ability for controlled drug release and chemical sensing applications.

Previous studies have successfully demonstrated the ability for EAP devices to manipulate single living cells for biotechnology applications [3, 4]. Similarly, Jager *et al* [5] fabricated a serially connected micromanipulator capable of grasping, moving and positioning 100 μm glass beads, thus showing the potential of EAP for single-cell manipulation. While the operation of EAP in specific aqueous electrolytes has received most attention, a few studies have shown their operation in non-aqueous environments. The ability for the latter will widen the potential for EAP applications and commercialization. Significant attempts have been directed towards the synthesis, performance quantification, positioning improvement and applications of non-aqueous polypyrrole (PPy) conducting polymer actuators with lengths greater than 5 mm [6–9], though to our knowledge there have been no reports on micron-sized all-solid-state polymer actuators. A primary reason for this is that the synthesis technique and structure of the dry-type actuators is not conducive to the use of conventional lithographic techniques for fabricating actuators less than 1 mm in length. For the design of solid-state, microactuators in this study, we employed our new hybrid microfabrication technique that uses a bottom-up approach to fabricate composite structures consisting of two electroactive polymer layers [9], and a top-down approach using an excimer laser ablation technique to produce microactuators [10, 11].

Stiffness characterization of the microactuators is critical for assessing their ability to withstand mechanical forces, and for knowing the forces that they themselves will apply to the external environment (e.g. when gripping an object). In this context, various methods used to determine the normal stiffness, or 'spring constant', of micron-sized silicon cantilevers used in atomic force microscopy (AFM) research [12] highlight the possibility of adapting such methods for calibrating similar sized EAP microactuators. This idea of applying AFM calibration techniques forms the basis of this study and specifically involves a modified approach of the reference spring method [14] to determine the spring constant of polypyrrole microactuators fabricated using our method described above. The reference spring method uses Hooke's law, $F = kD$, to calculate the spring constant, k, by pushing an AFM cantilever with unknown k against a reference cantilever (with known k), and then measuring the applied force, F, and resulting displacement, D, of the AFM cantilever. Due to its simple implementation, we found this method to be most amenable for our measurements in comparison to other AFM calibration techniques such as the added mass, thermal noise and Sader methods [13–15]. In principle, it may be possible to use these other techniques, though they were deemed less applicable due to their requirement for a direct measurement of the polymer microactuator displacement and/or the resonance frequency. For example, the former is required to obtain parameters such as the fundamental resonance frequency, thermal noise spectra and/or quality factor, and typically require a specially designed detection system (e.g. optical detection) for measurement of the beam displacement. For practical reasons, a detection system for the polymer microactuators was not employed in this study, while alternative attempts to use the AFM optical detection system by positioning the polymer microactuators in the AFM were unsuccessful. This was due to two reasons that included a lack of reflectivity from the surface of the polymer microactuator to generate a sufficient signal in the photodiode and the occurrence of an incorrect beam deflection angle for the optical path. In contrast to these other methods, the reference spring method provided a straightforward approach that relied only on a static measurement of the polymer microactuator displacement that could be measured indirectly with a standard silicon cantilever using the AFM.

We aimed to assess this AFM-based approach as an alternative to calculating the spring constant of polymer actuators based on their material properties, which is typically difficult due to their tri-composite structure. This composite structure makes it difficult to accurately model the effective elastic modulus due to the complexity of the interrelated individual material parameters that affect their bulk mechanical properties (e.g. actuation, Young's modulus, density). Accurate determination of their dimensions, i.e. using optical techniques, can be used to determine the spring constant from the Euler–Bernoulli model [16], though they may still be limited from non-isotropic properties in the composite material structure. A major problem has been the complex nature of the polymer actuation mechanisms and lack of analogous classical theories that have hindered the development and conclusive experimental verification of comprehensive 'electro-chemo-mechanical' models of the actuator behavior. Recently, the effective modulus of elasticity of the macro-sized tri-layer actuators was measured by modeling their material properties [17], though this method also required *a priori* measurement of the resonant frequency that may become problematic for polymer microactuators using current detection systems.

In AFM, an accurate measurement of the spring constant is of crucial importance for quantifying the surface force interactions between the probe tip and sample at sub-nanometer resolution (e.g. forces $< 10^{-10}$ N). This ability to measure such small forces with nanometer lateral precision underlies the AFM's unique strength and has significantly

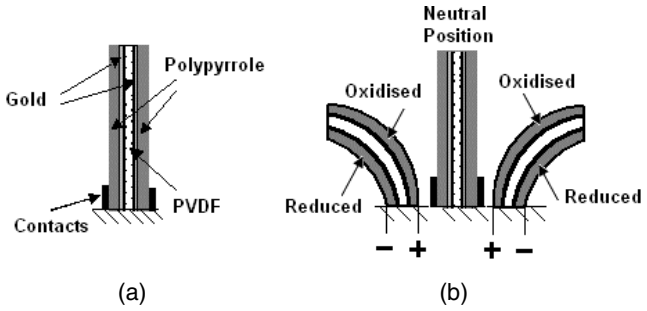

Figure 1. (a) Schematic structure of the conducting polymer actuator and (b) schematic representation of the bending principle. This actuator is anion-driven; the anions in the salt move into the positively charged electrode to cause a volume expansion. If it is cation-driven, the cations in the salt move into the negatively charged electrode to cause volume expansion, hence the bending direction will be from the negative electrode to the positive electrode—the opposite to what is shown in (b).

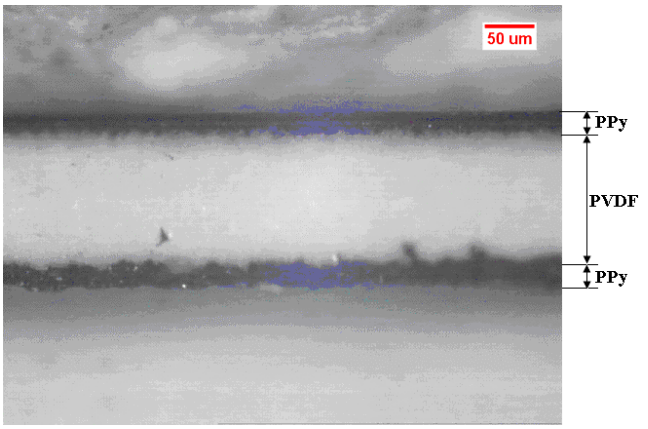

Figure 2. High resolution optical image of a side profile of the tri-layer solid-state PPy microactuator. The microactuator has dimensions 799 μm × 217 μm × 155 μm (length × width × thickness). The thickness of the PVDF layer (white section) is 127 μm and that of the outer PPy layers (black layers) is 14 μm. Thin layers of sputtered gold also exist between the PPy and PDVF layers.

impacted on numerous disciplines by quantifying fundamental surface forces (e.g. van der Waals) and biological inter/intra-molecular forces such as single ligand-receptor and protein interactions. With the further development of micro- and nanoactuators, a similar requirement for quantifying their surface force interactions is envisaged, particularly for chemical sensing and mechanical applications. Thus, as with AFM micron-sized cantilevers, standardized techniques with nanometer sensitivity must be implemented in order to characterize the mechanical properties (e.g. spring constant) of similar sized polymer actuators.

In this study, we utilized the highly sensitive optical lever detection system of an AFM, and ability to laterally position a probe with nanometer precision to apply a known load directly at the end of a non-aqueous polymer microactuator. By measuring the resulting displacement, the spring constant of the microactuator could easily be determined using approaches based on the reference spring calibration method. Importantly, this method was quick and simple (i.e. Hooke's law) and did not require prior information on the dimensions or elastic modulus of the polymer microactuators. Results revealed interesting changes in the spring constant when an electrical stimulus was applied to the microactuator during actuation.

2. Synthesis and operational principle of actuators

Figure 1 illustrates the fabricated structure of the polymer actuators used in this paper and outlines the actuation mechanisms for these non-aqueous solid-state actuators. The laminated structure behaves like a bilayer that generates a simple bending motion. In contrast to a single active polymer layer with uniform strain (i.e. no bending), the inclusion of a middle PVDF layer separating two polymer layers results in differential strain at each layer causing bending, as shown in figure 1. The synthesis of this structure starts with the sputter coating of gold particles (a thickness ranging between 10 and 100 Å) on both sides of a PVDF sheet (Millipore), which is like a filter membrane with a pore size of 0.45 μm and nominal thickness of 110 μm. The coated layers of gold serve to increase the conductivity of the polymer electrodes to be grown. Propylene carbonate (PC, Aldrich), lithium triflouromethanesulfonimide (Li^+TFSI^-, 3 M) were used as received. Pyrrole (Merck) was distilled and stored under nitrogen at −20 °C before use [9, 17].

Using a potentiostat/galvanostat (EG&G Princeton Applied Research Model 363), the polypyrrole (PPy) layers were grown galvanostatically on the gold-coated PVDF at a current density of 0.1 mA cm^{-2} for 12 h from the growth solution. The growth solution contained 0.1 M LiTFSI, 0.1 M pyrrole monomer and 1% water in PC that was stirred and degassed with N_2 for 15 min. With this growth time, the thickness of each polymer layer was approximately 30 μm. The deposition temperature was −33 °C and the synthesized bulk sheet was doped with $TFSI^-$ ions. Figure 2 shows a high resolution optical image of a side profile of the microactuator detailing the structure and dimensions of the layered composite material [11]. Upon completion of the polymerization, the polymer-coated bulk sheet was rinsed with acetone to remove any remaining growth solution and stored in the salt (LiTFSI) and solvent (PC) solution until it was needed for the AFM measurements.

The structure of the actuator with electrolyte stored in the PVDF membrane functions as an electrochemical cell and is electrically stimulated by applying a potential difference or passing current between the polymer electrodes via the contacts. The whole microactuator structure is charged like a capacitor. During oxidation (positive applied potential), the negatively charged $TFSI^-$ anions move towards the inside of the positively charged polymer electrode to maintain charge neutrality, and hence cause a volume expansion. At the opposing negatively charged polymer electrode, the ejection of the $TFSI^-$ anions during reduction causes a volume contraction. This differential volume change between the two polymer electrode layers results in the bending towards the negative electrode/cathode, as depicted in figure 1(b). Thus, volume changes in the polymer occur due to movement of

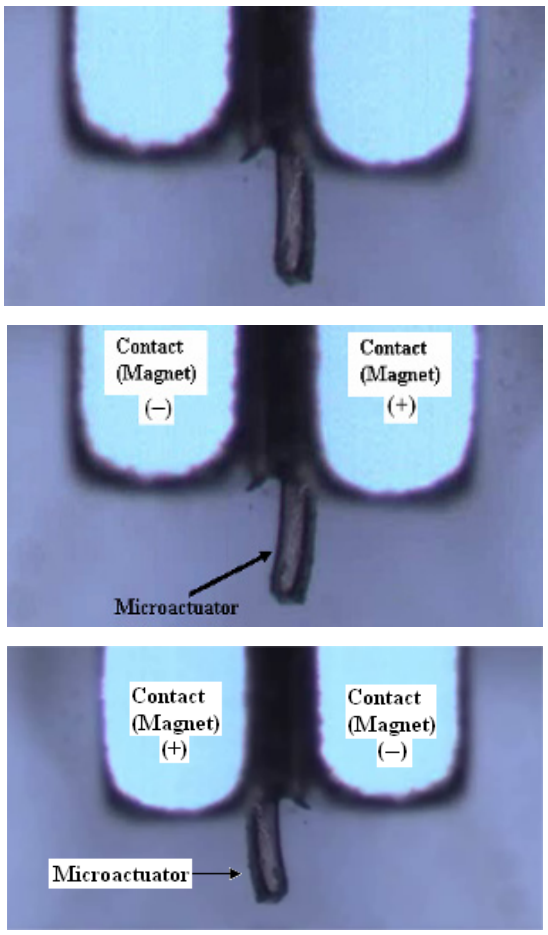

Figure 3. Optical images of a solid-state PPy microactuator. The above image shows the microactuator in its neutral position (0 mV). The middle image below shows the microactuator bending to the left when electrically activated with an applied potential of 1 V. When the polarities of the contacts are inverted, the actuator bends to the right. The microactuator is tightly clamped at its base by two permanent magnets on either side, which also make contact with two electrically conducting metal plates.

charge balancing anions in and out of the polymer layers. Figure 3 shows optical images of a PPy polymer microactuator in its neutral position without an applied potential and subsequently when it is bending due to electrical activation with an applied potential of ± 1 V. The incorporation of associated solvent molecules due to osmotic effects may also contribute to the volume changes, in addition to the bending electrostatic forces between the displaced ions and the polymer backbone that are also believed to contribute to the bending [19]. The actuation speed and overall volume change also depends on many electro-chemo-mechanical parameters, including the thickness of the polymer layers, the ion type and sizes, charge injected (potential applied), the ionic concentration, the solvent, and the width of the actuator [9, 18].

3. Stiffness models for polymer actuators

The internally induced actuation or bending force of the microactuator due to movement of ions in and out of the polymer layers is analogous to a uniformly distributed load acting on a cantilever beam due to the fact that the actuation ability happens along the thickness of the polymer layers [18]. According to linear beam theorem, the tip deflection of the beam under the uniformly distributed load is [18, 22]

$$y = \frac{FL^3}{24EI}(8 - 6\lambda + \lambda^3), \qquad \text{where } \lambda = \frac{L_a}{L} \quad \text{and} \quad F = L_a f_a. \tag{1}$$

With reference to figure 4(b), $L_a = L$ or $\lambda = 1$ for our microactuators. From equation (1), the stiffness of the beam is

$$k = 8\frac{EI}{L^3} \tag{2}$$

where $EI = 2b(\frac{h_1^3}{3}E_{pvdf} + \frac{h_2^3 - h_1^3}{3}E_{ppy})$, which is the flexural rigidity of the microactuators, and E_{ppy} and E_{pvdf} are the elastic modules of the PPy and PVDF, respectively. A description of the remaining parameters is provided in figure 4.

From equation (2), the stiffness constant is inversely proportional to the cube of the length, and linearly proportional to the actuator width and to the cube of the actuator thickness. This model can provide an estimation of spring constant for the microactuators; however, it does not account for dynamic changes in the elastic modulus of the PPy and PDVF layers which can occur during the actuation process. In particular, this situation is compounded by the large number of variables and interrelated parameters that can affect the actuation process, and therefore also the material properties of the tri-composite microactuator structure [19]. Previous studies on polymer actuators have also used a direct measurement of the resonant frequency to calculate the resultant modulus of elasticity from the following expression [17]:

$$k = 9.3056\, m\omega_n^2 \tag{3}$$

where $m = 2Lbh_1\rho_{pvdf} + 2Lb(h_2 - h_1)\rho_{ppy}$ and the first resonant frequency ω_n is in hertz. This method also necessitates accurate measurements of the actuator dimensions and resonant frequency, as well as the PPy and PVDF densities (ρ_{ppy}, ρ_{pvdf}) when they are a part of the tri-layer microactuators.

In addition to the above models, there are several AFM calibration techniques that appear feasible for calculating the spring constant of the polymer microactuators, though they have yet to been tested. For example, the Sader method requires only a measurement of the resonant frequency, quality factor and plan view dimensions of the cantilever. Furthermore, it does not require information on the mass or density properties of the actuator materials. It is noted that this method is valid for cantilever beams where the aspect ratio is >3 and the quality factor greatly exceeds $\gg 1$ [15]. Another method is the parallel fluid flow method that is based on measuring the changes in the resonance frequency of the cantilever, while a fluid in a microchannel flows parallel to both sides of the cantilever [21]. This method must be implemented in a fluid cell and requires the density and viscosity of the fluid, the accurate dimensions of the microchannel, and the resonance frequencies of the cantilever in and out of the fluid.

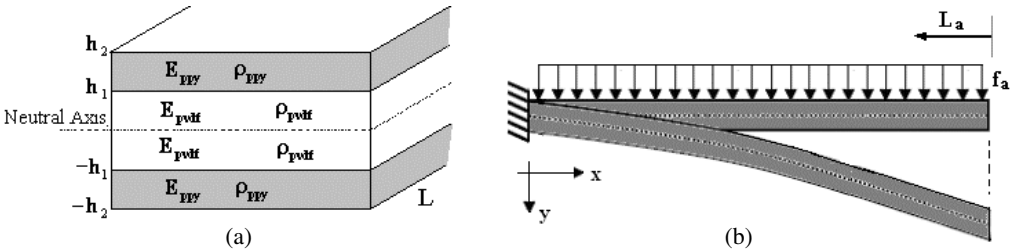

Figure 4. Description of the geometric parameters to formulate the stiffness model of the tri-layer polymer actuators.

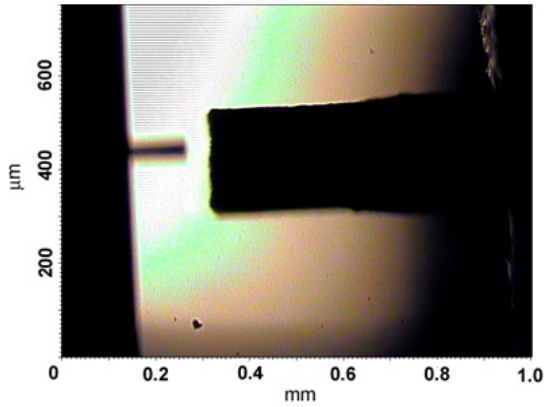

Figure 5. Optical image showing the polymer microactuator relative to the silicon AFM cantilever under the AFM.

4. Methods—reference spring calibration

In this study, we wanted to assess an alternative approach based on the reference spring method implemented by Torii *et al* [14], which specifically involved pushing an AFM cantilever with unknown spring constant onto a large scale 1 cm pre-calibrated reference cantilever. Importantly, this approach provided a direct measurement of the spring constant and circumvented the need to know the material properties, dimensions and/or resonant frequency of the polymer microactuator. An optical top-down view of the AFM measurement and schematic diagram describing how the spring constant is measured is shown in figures 5 and 6, respectively. Prior to the stiffness estimation of the microactuator, the spring constant of the AFM cantilever, k_C, used in the experiments was pre-calibrated using the thermal calibration method [14]. For this initial calibration, the inverse lever optical sensitivity (InvOLS) was measured for the AFM cantilever by taking a force versus distance curve on a non-compliant surface (i.e. glass slide). The slope of the contact region in these curves represented the InvOLS (nm V^{-1}) and was used to convert the photodiode voltage cantilever deflection signal into a distance given in meters (typically 10^{-9} m). The AFM cantilever was then pushed against the end of the polymer microactuator with a known force, F_C, by performing a force versus distance curve and the resulting deflection of the AFM cantilever, ΔD_C, was recorded using the optical detection system of the AFM.

The applied force on the polymer microactuator actuator, F_A, is equivalent to the applied force of the AFM cantilever:

$$F_C = F_A. \tag{4}$$

Incorporating Hooke's law into equation (4) gives

$$k_C \Delta D_C = k_A \Delta D_A \tag{5}$$

where k_A and ΔD_A are the spring constant and deflection of the polymer microactuator, respectively.

During the force measurement, the vertical displacement of the piezo, ΔD_P, in the contact region of the force curve represents the combined deflection of the AFM cantilever tip and polymer microactuator. Thus the latter is given by

$$\Delta D_A = \Delta D_P - \Delta D_C. \tag{6}$$

Substituting equation (6) into equation (4) then gives the spring constant of the polymer microactuator as the unknown parameter, where

$$k_C \Delta D_C = k_A (\Delta D_P - \Delta D_C). \tag{7}$$

Dividing equation (7) by the vertical displacement of the piezo, ΔD_P, and also substituting the slope of the contact region of the force curve, S, where

$$S = \frac{\Delta D_C}{\Delta D_P} \tag{8}$$

gives the final form (8), whereby the spring constant of the polymer microactuator can be obtained by knowing the spring constant of the AFM cantilever and slope of the force curve:

$$k_A = \frac{k_C S}{1 - S}. \tag{9}$$

It is noted that, to minimize errors associated with torsional bending and progressive stiffness changes, as measurements are made along the length of the polymer actuator, the AFM cantilever was positioned directly in the middle and as close to the end of the actuator using the optical capabilities shown in figure 5. Additional errors are also expected to arise due to the error in the pre-determined spring constant of the AFM cantilever ($\approx$<10%). It was also ensured that the estimated spring constant of the polymer actuator, k_A, to be measured was in the range $0.3k_C < k_A < 3k_C$ such that the deflection signal measured was not dominated by one of the cantilever beams. Overall errors associated with limitations of

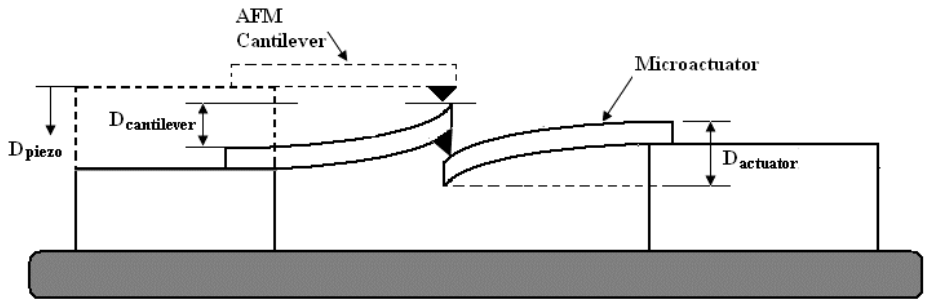

Figure 6. Schematic representation of the measurement system (not to scale).

the reference spring method have previously been reported to be <10–20%.

An important consideration for our measurements was the potential for the tip indentation of the polymer actuator due to the lower elastic modulus of the PPy (∼80 MPa) and PVDF (∼300 MPa) beam material compared to silicon/silicon nitride (150–300 GPa), which is commonly used for fabrication of AFM cantilevers. To address this situation, we performed a series of force measurements at different applied loads to assess at which point linear constant compliance in the slope of the force curve had been achieved. A constant compliance region is essential for the spring constant calibration procedure, as it represents both the deflection of the AFM cantilever and polymer actuator rather than contributions from indentations of the actuator material.

The force measurements were taken with a Mikromach NSC cantilever using an MFP-3D AFM (Asylum Research, Santa Barbara, CA). The spring constant of the AFM cantilever was calibrated to be 43 N m^{-1} and the measured InvOLS was 47.7 nm V^{-1}. A series of at least 10 force curves were taken at different applied loads of 100, 200, 300, 400, 500 and 700 nN. Force curves were performed with a scan rate and z distance of 0.5 Hz and 350 nm, respectively. Measurements were first made on the microactuator in its neutral position (no applied potential) and then with an applied potential of −500 and +500 mV. The application of the negative and positive potentials caused bending of the actuator in the upward and downward directions, respectively, and it was observed that the force curves were stable during these measurements. Measurements were made on a polymer microactuator with the length, width and thickness dimensions described above.

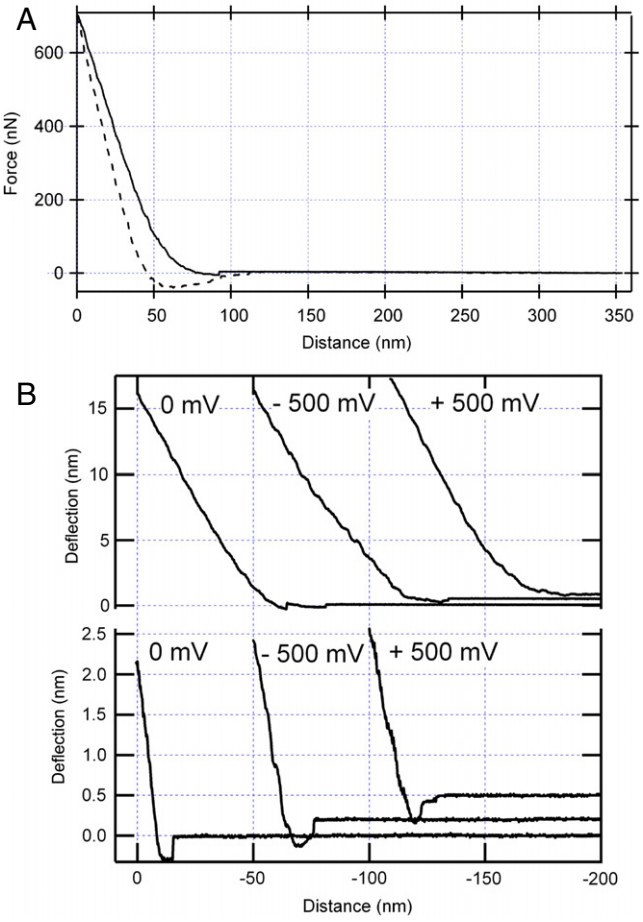

Figure 7. (A) Force measurement taken on the polymer microactuator in the neutral position (0 V) showing both the approach (solid line) and retraction (dashed line) curves. The applied load was 700 nN. (B) Force curves taken on the neutral and electrically activated states at applied loads of 100 nN (below) and 700 nN (above).

5. Results and discussion

Figure 7(A) shows a typical force curve taken at the end of the polymer microactuator without the application of an applied voltage (i.e. in its neutral position). The extension curve (solid curve) showed a small attractive force before contact, followed by a nonlinear increase in the force, until a linear constant compliance region was reached at ≈200 nN. Upon retraction (dashed curve), the hysteresis between the curves indicated that the actuator had not fully recovered to its neutral position during the timescale of the measurement. An adhesive pull-off force was also observed in the retraction curve and corresponded to the force required to overcome the initial attractive force during the approach.

The nonlinear region in the contact region of the force curve indicated an expected contribution from tip indentation of the polymer actuator material. In this case, $\Delta D_{\mathrm{P}} \neq \Delta D_{\mathrm{A}} + \Delta D_{\mathrm{C}}$, but which actually includes a contribution from the indentation, ΔD_{I}. This additional contribution of ΔD_{I} causes an increase in the change of ΔD_{P} relative to ΔD_{C}, which

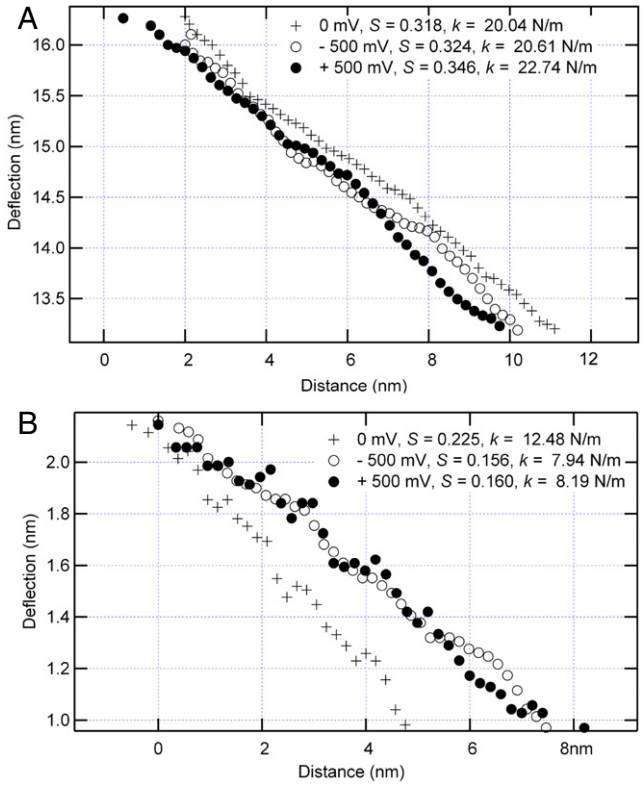

Figure 8. Linear fitted region of the slope in the contact region of representative curves at applied loads of 700 nN (A) and 100 nN (B) for both the neutral and electrically activated states of the polymer microactuator.

results in a nonlinear force profile with a smaller gradient of slope. Thus, if ΔD_{I} is not considered when measuring the slope, S, from the contact region of the curve, then the effective ΔD_{A} will be overestimated and result in the underestimation of the spring constant, k_{A}, and what would appear to be a more compliant cantilever. As the applied load increases to ≈200 nN, there is a transition to a linear constant compliance region, indicating that ΔD_{P} primarily represents the deflection of the AFM cantilever and polymer actuator, as given in a rearrangement of equation (6). This region of the force curve can be used to obtain an accurate measurement of the slope, S, and is also an essential criteria when measuring the inverse optical lever sensitivity (invOLS) of the AFM cantilever for force measurements in general.

Figure 7(B) shows representative extension curves for measurements taken on the polymer microactuator with an applied potential of 0 mV (neutral position), −500 mV and +500 mV. The force curves shown were taken at two different applied loads of 100 and 700 nN. For both the neutral and electrically activated states, the force measurements were stable and showed a similar force profile to that described above in figure 7(A). To calculate the slope, S, of the curves shown in figure 7(B), a linear fit was applied to a portion of the contact region positioned near the top part of the curve at the maximum applied load. A closer inspection of this fitted portion of the curve for each condition and the corresponding slope values and calculated k values from

Table 1. Estimated stiffness constants when the microactuator was not activated, i.e. passive.

Applied force, F (nN)	Mean of stiffness, k_{mean} (N m^{-1})	Standard error, SE
100	13.30	0.69
200	16.99	1.27
300	17.79	0.71
400	18.02	1.06
500	17.19	1.50
700	19.22	0.24

Table 2. Estimated stiffness constants when the microactuator was activated with +500 mV.

Applied force, F (nN)	Mean of stiffness, k_{mean} (N m^{-1})	Standard error, SE
100	7.89	0.32
200	14.25	0.65
300	17.463	1.12
400	22.87	1.05
500	21.28	1.53
700	22.81	0.87

Table 3. Estimated stiffness constants when the microactuator was activated with −500 mV.

Applied force, F (nN)	Mean of stiffness, k_{mean} (N m^{-1})	Standard error, SE
100	7.85	0.45
200	13.99	0.87
300	18.41	1.17
400	19.96	0.64
500	20.56	1.12
700	20.07	0.87

equation (9) are compared for representative curves in figure 8. At an applied load of 700 nN (maximum $\Delta D_{\mathrm{C}} = \approx$16 nm), the slope and k values for both the neutral and electrically activated states showed no significant difference considering the given experimental error of the calibration technique. This is qualitatively shown by the superimposition of each curve in figure 8. In contrast, for the applied load 100 nN (maximum $\Delta D_{\mathrm{C}} = \approx$2 nm), the electrically activated states showed significantly lower slope and subsequent k values compared to the neutral state. Mean k values at each of the different applied loads (from 10 curves) were calculated using the same approach and are shown for each condition (i.e. 0 mV, −500 mV, +500 mV) in tables 1–3.

For the neutral state, table 1 shows that the k value increased with an increase in the applied load value up to approximately 200 nN, indicating that the measured slope value also increased due to the decreasing contribution from the tip–sample indentation, ΔD_{I} (i.e. the beam material becomes less compressible). Beyond this force region, the k values became constant, indicating that the slope had reached constant compliance and ΔD_{C} was primarily due to the coordinated deflection of the polymer microactuator and AFM cantilever. Similarly for the activated states, tables 1 and 2 show that the k values continued to increase until higher applied loads of 400 nN, upon which they also became

constant at the remaining applied loads. As the constant compliance region is a requirement for the reference spring constant calibration method, the magnitude of the constant k values in tables 1–3 reflects the actual measured spring constant of the polymer microactuator under each condition. Thus, the mean k values from the constant compliance region (i.e. region $>$ 400 nN) of the neutral and electrically activated states were 18.14 N m^{-1} (neutral), 22.32 N nm^{-1} (+500 mV) and 20.19 N m^{-1} (−500 mV), indicating that the k values for the activated states were similar, although they appeared to be slightly higher than the neutral state. In contrast to reference spring calibration measurements on typical AFM cantilevers and potential silicon MEMS devices, our measurements highlight the need to ensure that a constant compliance region is achieved in measurements for polymer microactuators or any cantilever design in general that is fabricated using a softer, deformable material.

Tables 1–3 also show that the k values for the activated states were significantly less than the neutral state at lower applied loads, particularly at 100 nN where the values almost differed by ≈50%. This observation indicated that the contribution from ΔD_{I} was greater for the former at these applied loads, suggesting that the elastic modulus of the material, most likely the PPy layer directly in contact with the AFM tip, decreased when the polymer microactuator was electrically activated. This situation is confirmed in previous AFM studies that have utilized contact mechanical models (e.g. Hertz, JKR, DMT models) to describe the relationship between the AFM tip indentation, ΔD_{I}, and elastic modulus of a material deformed under an applied load during a force measurement. In these cases, an increase in ΔD_{I} essentially gives rise to a lower elastic modulus. The decrease in the material stiffness for the electrically activated polymer microactuator is not unexpected as the Young's modulus of PPy conducting films has been shown to change dramatically by up to 50–400% during oxidation/reduction due to modifications in the polymer backbone and/or plasticization effects from the incorporation of solvent. We also note that high resolution video microscopy of the side profile of our polymer microactuators, as shown in figure 2, appears to reveal the accumulation of solvent in the PDVF and PPy layers during actuation, in addition to a simple visual inspection that shows an increase in wetness at their surface.

Interestingly, according to the stiffness models described above, a decrease in the elastic modulus of the PVDF/PPy tri-composite material within a microactuator of the same dimensions should result in a decrease in the spring constant compared to the neutral state. However, the comparable k values of both the neutral (18.14 N m^{-1}) and activated states (22.32 N nm^{-1}, +500 mV; 20.19 N m^{-1}, +500 mV) suggests that the potential stiffness decrease due to the change in the elastic modulus is compensated by a resistant effect from the electrical activation of the polymer microactuator. This can be explained by the effect of electrical activation that manifests itself as an increase in mechanical energy by charging the polymer microactuator and increasing its apparent stiffness. It is possible that, during the application of a DC voltage, irrespective of the polarity, the observed stiffness increase arises from an antagonistic effect by the polymer microactuator as the AFM cantilever pushes against it.

A potential application of microcantilevers in MEMS is their operation as an active electrostatic microswitch. For these devices, there is a need to know the stiffness of the microcantilever in order to model and estimate the pull-in voltage, as the microcantilever is attracted to the surface upon the application of a DC voltage across the switch [20]. To prevent pull-in instabilities associated with attractive forces, the pull-in voltage of the microcantilever can be determined *a priori* by knowing the spring constant, where the pull-in voltage V_{PI} is given by equation (10). Hence, this makes sure that the spring force is always greater than the attractive electrostatic force:

$$V_{\mathrm{PI}} = \sqrt{\frac{8K_{\mathrm{eff}}d_0^3}{27\varepsilon_0 A_{\mathrm{eff}}}} \tag{10}$$

where d_0, ε_0, K_{eff}, and A_{eff} are the zero-voltage gap spacing between two parallel conductive plates forming a capacitor, the permittivity of space between the plates, the spring constant of the compliant structure holding the top plate and the effective area between the two plates, respectively [20]. The spring constant for MEMS switches should be between 5 and 40 N m^{-1}, which encompasses the neutral and electrically activated stiffness of our polymer microactuators, and can now be determined directly using the method outlined in this study. Furthermore, the use of EAP microactuators as microswitches could overcome the problem of surface adhesion instabilities due to its built-in actuation mechanism. In other applications such as biotechnology, single-cell probing and manipulations must be performed using controlled forces so as not to damage cells. Thus this calibration technique will also assist in the design of polymer microactuators for these bio-applications.

6. Conclusions

The normal stiffness of a conducting polymer microactuator has been characterized using an AFM-based spring constant calibration technique. A number of conclusions can be drawn from this study, including:

- The importance of evaluating that constant compliance has been achieved in reference spring calibration measurements on polymer microactuators and other microcantilevers fabricated from soft, deformable materials.
- The calibrated spring constant k of both the neutral and activated polymer microactuators with dimensions of 799 μm × 217 μm × 155 μm (length × width × thickness) were ≈ in the range of 20 N m^{-1}.
- The stiffness of the PDVF/PPy surface layers decreased in the electrically activated microactuators, most likely due to plasticization effects as a result of an increased uptake of solvent. However, the measured spring constant k of these electroactive microactuators was similar to the neutral state, suggesting that the expected decrease in stiffness due to the plasticization was offset by other mechanisms due to the electrical activation (e.g. resistance effects).

In conclusion, the method used in this study is simple, versatile and easy to implement to determine the spring constant of polymer microactuators. In contrast to traditional mechanical models, this method provides a direct measurement of k and alleviates problems associated with the dynamic redox properties changes (e.g. Young's modulus) during electrical activation in these systems. Further work applying other calibration techniques is currently in progress for validation purposes and the use of ionic liquids as an alternative electrolyte is also being considered to remove plasticization and solvent-related effects. Along with our previous work [11], this study highlights the first solid-state conducting polymer actuators with built-in actuation ability for operation in aqueous and non-aqueous media. The ability to determine their normal stiffness provides an important step in their specific design for a numerous range of applications, including micromanipulation of living cells, bio-analytical nanosystems, data storage, lab-on-chip, microvalve, microswitch, microshutter, cantilever light modulators, micro-optical instrumentation, to artificial muscles for macro-and micro-robotic manipulation devices.

Acknowledgments

The authors thank Professor John Sader of the University of Melbourne for his insightful comments and suggestions on this work. This work was supported in part by an ARC Discovery Project (DP0878931) and ARC Centre of Excellence for Electromaterials Science (CE0561616).

References

[1] Ataka M A, Omodaka A, Takeshima N and Fujita H 1993 Fabrication and operation of polyimide bimorph actuators for a ciliary motion system *J. Microelectromech. Syst.* **2** 146

[2] Kim D H *et al* 2005 A superelastic alloy microgripper with embedded electromagnetic actuators and piezoelectric force sensors: a numerical and experimental study *Smart Mater. Struct.* **14** 1265–72

[3] Smela E 1999 Microfabrication of PPy microactuators and other conjugated polymer devices *J. Micromech. Microeng.* **9** 1–18

[4] Jager E W H, Smela E and Inganas O 2000 Microfabricating conjugated polymer actuators *Science* **290** 1540–5

[5] Jager E W H, Inganas O and Lunstrom I 2000 Microrobots for micrometer-size objects in aqueous media: potential tools for single cell manipulation *Science* **288** 2335–8

[6] Alici G and Huynh N N 2007 Performance quantification of conducting polymer actuators for real applications: a microgripping system *IEEE/ASME Trans. Mechatronics* **12** 73–84

[7] Alici G, Spinks G M, Huynh N N, Sarmadi L and Minato R 2007 Establishment of a biomimetic device based on tri-layer polymer actuators—propulsion fins *J. Bioinspir. Biomim.* **2** S18–30

[8] Yao Q, Alici G and Spinks G M 2008 Feedback control of tri-layer polymer actuators to improve their positioning ability and speed of response *Sensors Actuators* A **144** 176–84

[9] Wu Y, Alici G, Spinks G M and Wallace G G 2006 Fast tri-layer polypyrrole bending actuators for high speed applications *Synth. Met.* **156** 1017–22

[10] Dyer P E 2003 Excimer laser polymer ablation: twenty years on *Appl. Phys.* A **77** 167–73

[11] Alici G, Devaud V, Renaud P and Spinks G M 2009 Conducting polymer microactuators operating in air *J. Micromech. Microeng.* **19** 025017

[12] Butt H J, Cappella B and Kappl M 2005 Force measurements with the atomic force microscope: technique, interpretation and applications *Surf. Sci. Rep.* **59** 1–152

[13] Clifford C A and Seah M P 2005 The determination of atomic force microscope cantilever spring constants via dimensional methods for nanomechanical analysis *Nanotechnology* **16** 1666–80

[14] Torii A, Sasaki M, Hane K and Okuma S 1996 A method for determining the spring constant of cantilevers for atomic force microscopy *Meas. Sci. Technol.* **7** 179–84

[15] Sader J E, Chon J W M and Mulvaney P 1999 Calibration of rectangular atomic force microscope cantilevers *Rev. Sci. Instrum.* **70** 3967–9

[16] Frisch-Fay R 1962 *Flexible Bars* (London: Butterworth)

[17] John S W, Alici G and Cook C D 2008 Validation of a resonant frequency model for polypyrrole trilayer actuators *IEEE/ASME Trans. Mechatronics* **13** 401–9

[18] Alici G, Metz P and Spinks G M 2006 A methodology towards geometry optimisation of high performance polypyrrole (PPy) actuators *J. Smart Mater. Struct.* **15** 243–52

[19] Alici G, Mui B and Cook C 2006 Bending modeling and its experimental verification for conducting polymer actuators dedicated to manipulation applications *Sensors Actuators* A **126** 396–404

[20] Pamidighantam S, Puers R, Baert K and Tilmans H A C 2002 Pull-in voltage analysis of electrostatically actuated beam structures with fixed-fixed and fixed-free end conditions *J. Micromech. Microeng.* **12** 458–64

[21] Lubarsky G V and Hahner G 2008 Hydrodynamic methods for calibrating the normal spring constant of the microcantilevers *Nanotechnology* **19** 325707

[22] Roark R J and Young W C 1989 *Formulas for Stress and Strain* (New York: McGraw-Hill)